

ortho-Metallated complexes of platinum(II) and diplatinum(I) containing the carbanions (2-diphenylphosphino)phenyl and (2-diphenylphosphino)-*n*-tolyl (*n* = 5, 6)

Martin A. Bennett,^{*a} Suresh K. Bhargava,^{*b} Johannes Messelhäuser,^a Steven H. Privér,^b Lee L. Welling^a and Anthony C. Willis^a

Received 26th February 2007, Accepted 9th May 2007

First published as an Advance Article on the web 31st May 2007

DOI: 10.1039/b702808c

When the *ortho*-metallated complexes cis -[Pt(κ^2 -C₆H₃-5-R-2-PPh₂)₂] (R = H **1**, Me **2**) are either heated in toluene or treated with CO at room temperature, one of the four-membered chelate rings is opened irreversibly to give dinuclear isomers [Pt₂(κ^2 -C₆H₃-5-R-2-PPh₂)₂(μ -C₆H₃-5-R-2-PPh₂)₂] (R = H **10**, Me **11**). A single-crystal X-ray diffraction study shows the Pt...Pt separation in **10** to be 3.3875(4) Å. By-products of the reactions of **1** and **2** with CO are polymeric isomers (R = H **13**, Me **14**) in which one of the P–C ligands is believed to bridge adjacent platinum atoms intermolecularly. In contrast to the behaviour of **1** and **2**, when cis -[Pt(κ^2 -C₆H₃-6-Me-2-PPh₂)₂] (*cis*-**3**) is heated in toluene, the main product is *trans*-**3**, and reaction of *cis*-**3** with CO gives a carbonyl complex [Pt(CO)(κ^1 -C-C₆H₃-6-Me-2-PPh₂)(κ^2 -C₆H₃-6-Me-2-PPh₂)] **15**, in which one of the carbanions is coordinated only through the carbon. Formation of a dimer analogous to **10** or **11** is sterically hindered by the 6-methyl substituent. Comproportionation of **1** or **2** with [Pt(PPh₃)₂L] (L = PPh₃, C₂H₄) gives diplatinum(I) complexes [Pt₂(μ -C₆H₃-5-R-2-PPh₂)₂(PPh₃)₂] (R = H **16**, Me **17**). An X-ray diffraction study shows that **17** contains a pair of planar-coordinated metal atoms separated by 2.61762(16) Å. There is no evidence for the formation of an analogue containing μ -C₆H₃-6-Me-2-PPh₂. The axial PPh₃ ligands of **16** are readily replaced by BuⁿNC giving [Pt₂(μ -2-C₆H₄PPh₂)₂(CNBuⁿ)₂] **18**, which is protonated by HBF₄ to form a μ -hydridodiplatinum(II) salt [Pt₂(μ -H)(μ -2-C₆H₄PPh₂)₂(CNBuⁿ)₂]BF₄ [**21**]BF₄. The J_{PtPt} values in [**21**]BF₄ and **18**, 2700 Hz and 4421 Hz, respectively, reflect the weakening of the Pt–Pt interaction caused by protonation. Similarly, **16** and **17** react with the electrophiles iodine and strong acids to give salts of general formula [Pt₂(μ -Z)(μ -C₆H₃-5-R-2-PPh₂)₂(PPh₃)₂]Y (Y = Z = I, R = H **19**⁺, Me **20**⁺; Z = H, Y = BF₄, PF₆, OTf, R = H **22**⁺; Z = H, Y = PF₆, R = Me **23**⁺). A single-crystal X-ray diffraction study of [**23**]PF₆ shows that the cation has an approximately A-frame geometry, with a Pt...Pt separation of 2.7888(3) Å and a Pt–H bond length of 1.62(1) Å, and that the 5-methyl substituents have undergone partial exchange with the 4-hydrogen atoms of the PPh₂ groups of the bridging carbanion. The latter observation indicates that the added proton of [**23**]⁺ undergoes a reversible reductive elimination–oxidative addition sequence with the Pt–C(aryl) bonds.

Introduction

The bifunctional, carbanionic ligand [2-C₆H₄PPh₂][−] is most often generated by C–H activation (*ortho*-metallation) of triphenylphosphine in its complexes of the later d-block elements. Although it behaves mostly as a chelate (κ^2P,C) ligand, forming a four-membered ring, there are well-established examples of bridging behaviour (μ - $\kappa P\kappa C$), and of interconversion between the two modes.¹

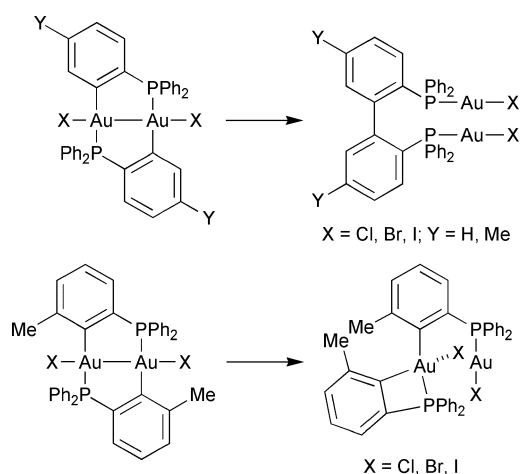
We have previously employed transmetalation from the organolithium reagent 2-LiC₆H₄PPh₂ to prepare chelate complexes of platinum(II) and rhodium(III), [M(κ^2 -2-C₆H₄PPh₂)_n] (M = Pt, *n* = 2; M = Rh, *n* = 3)^{2,3} and a binuclear gold(I) complex, [Au₂(μ -2-C₆H₄PPh₂)₂], in which the bridging *ortho*-metallated units and the

gold atoms comprise an eight-membered ring.^{4,5} These complexes are not accessible by *ortho*-metallation of PPh₃. We have also shown that substitution of a methyl group in the 6-position, *ortho* to the gold-carbon bond, of [Au₂(μ -2-C₆H₄PPh₂)₂] exerts a marked effect on the course of oxidative addition reactions with halogens. Whereas the dihalodigold(II) complexes [Au₂X₂(μ -C₆H₃-5-R-2-Ph₂)₂] (X = Cl, Br, I; R = H, Me) rearrange by coupling of the *o*-phenylene residues to give P-bonded digold(I) complexes [Au₂X₂{ μ -2,2'-Ph₂P(5,5'-R₂C₆H₃C₆H₃)PPh₂}],^{5–7} the digold(II) complexes in the 6-methyl series, [Au₂X₂(μ -C₆H₃-6-Me-2-Ph₂)₂], isomerise rapidly to gold(I)–gold(III) complexes in which one of the cyclometallated ligands is chelated to gold(III) (Scheme 1).⁷ No C–C coupling is observed in the 6-methyl series, presumably because steric repulsion between the methyl groups raises the energy of the transition state to reductive elimination of the two aryl groups.⁸

In view of these results, we wondered whether 5- or 6-methyl substitution would influence, electronically or sterically,

^aResearch School of Chemistry, Australian National University, Canberra, ACT 0200, Australia

^bSchool of Applied Sciences (Applied Chemistry), RMIT University, GPO Box 2476V, Melbourne, Victoria 3001, Australia



Scheme 1

the chemistry of $[\text{Pt}(\kappa^2\text{-C}_6\text{H}_4\text{PPh}_2)_2]$ **1**.^{2,3} The results are reported here, together with more details of the chemistry of **1**.

Results and discussion

Analogous to the previously reported preparation of $[\text{Pt}(\kappa^2\text{-C}_6\text{H}_4\text{PPh}_2)_2]$ **1**,^{8,9} treatment of the lithio-derivatives $\text{LiC}_6\text{H}_3\text{-5-Me-2-PPh}_2$ and $\text{LiC}_6\text{H}_3\text{-6-Me-2-PPh}_2$ with $[\text{PtCl}_2(\text{SEt}_2)_2]$ gave the corresponding bis(chelate) complexes $\text{cis-}[\text{Pt}(\kappa^2\text{-C}_6\text{H}_3\text{-}n\text{-Me-2-PPh}_2)_2]$ ($n = 5$ **2**; $n = 6$ **3**) as colourless, air- and moisture-stable solids in yields of ca. 80% and 50%, respectively. The IR spectra of **2** and **3**, like that of **1**, show bands characteristic of *ortho*-metallated PPh_3 complexes at ca. 1560 and 725 cm^{-1} ,⁹⁻¹¹ and the EI-mass spectra both show the same parent-ion peak. The ^{31}P NMR spectra of **2** and **3** consist of singlets with ^{195}Pt satellites at $\delta -52.5$ ($J_{\text{PtP}} 1352$ Hz) and -62.9 ($J_{\text{PtP}} 1370$ Hz), respectively, the parameters for **2** being almost identical with those previously reported for **1**. The shieldings are characteristic of ^{31}P nuclei in

four-membered chelate rings;¹² the coupling constants are lower than the expected value of 1800–2100 Hz for P *trans* to σ -aryl in planar platinum(II) complexes,^{13,14} presumably as a consequence of ring strain.

The solid state ^{31}P NMR spectrum of **2** shows two overlapping singlets of almost equal intensity, with ^{195}Pt satellites, at $\delta -53.2$ ($J_{\text{PtP}} 1362$ Hz) and -54.5 ($J_{\text{PtP}} 1355$ Hz), which presumably correspond to the crystallographically inequivalent phosphorus atoms observed in the X-ray structure (see below). Similar observations of inequivalent phosphorus resonances in solid state ^{31}P NMR spectra have been made for $\text{cis-}[\text{PtCl}_2\{\text{Ph}_2(\text{CH}_2)_n\text{PPh}_2\}]$ ($n = 1\text{--}5$)¹⁵ and $\text{cis-}[\text{PtCl}_2(\text{PPh}_3)_2]$.¹⁶

The presence of two four-membered chelate rings in **2** and **3** has been confirmed by single-crystal X-ray structural analysis. The molecular structures are shown in Fig. 1 together with selected bond lengths and angles. The coordination about platinum in both complexes is distorted square planar. In **3** the *ortho*-methyl substituents lie above and below the P–Pt–P plane. The Pt–C distance in **3** [2.095(3) Å] is slightly greater than those in **2** [2.062(3) Å, 2.058(4) Å] and **1** [2.063(2) Å], presumably because of steric crowding by the *ortho*-methyl groups; the Pt–P distances in **3** [2.2799(8) Å], **2** [2.306(1) Å, 2.3034(9) Å] and **1** [2.297(1) Å] do not differ significantly. The bite angles of the chelate ligands in **1–3** are within the range 68–69° that is typical of *ortho*-metallated PPh_3 complexes.¹ However, the C–Pt–C angle in **3** (111°) is slightly greater than those in **1** and **2** (106°, 105°), and the P–Pt–P angle in **3** (113°) is correspondingly less than that in **1** and **2** (116°, 117°).

Oxidative addition reactions of **2** and **3**

These are summarised in Scheme 2. Like complex **1**, **2** reacts with one equivalent each of Cl_2 (*via* PhICl_2), Br_2 and I_2 , and with an excess of MeI , to give the platinum(IV) oxidative addition products $[\text{PtXY}(\kappa^2\text{-C}_6\text{H}_3\text{-}n\text{-Me-2-PPh}_2)_2]$ ($X = Y = \text{Cl}$ **4**, Br **5**, I **6**; $X = \text{Me}$, $Y = \text{I}$ **7**), most of which have been isolated and characterised by elemental analysis, EI-mass spectroscopy and NMR spectroscopy. The ^{31}P NMR data (see Experimental) serve

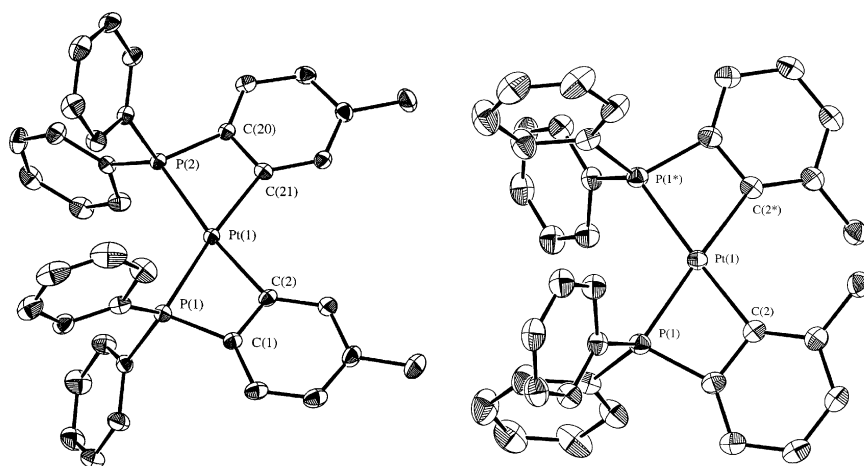
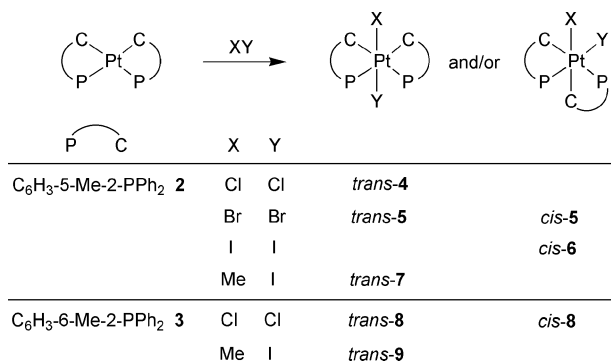


Fig. 1 Molecular structures of $\text{cis-}[\text{Pt}(\kappa^2\text{-C}_6\text{H}_3\text{-}n\text{-Me-2-PPh}_2)_2]$, $n = 5$ (**2**), 6 (**3**). Ellipsoids show 30% probability levels and hydrogen atoms have been deleted for clarity. Asterisks indicate atoms generated by crystallographic symmetry ($1 - x, y, \frac{1}{2} - z$). Selected bond lengths (Å) and angles (°): **2**: Pt(1)–P(1) 2.306(1), Pt(1)–P(2) 2.3034(9), Pt(1)–C(2) 2.062(3), Pt(1)–C(21) 2.058(4), P(1)–Pt(1)–C(2) 68.9(1), P(2)–Pt(1)–C(21) 68.6(1), P(1)–Pt(1)–C(21) 173.8(1), P(2)–Pt(1)–C(2) 173.7(1), P(1)–Pt(1)–P(2) 117.37(3), C(2)–Pt(1)–C(21) 105.1(1). **3**: Pt(1)–P(1) 2.2799(8), Pt(1)–C(2) 2.095(3), P(1)–Pt(1)–C(2) 68.44(9), P(1)–Pt(1)–C(2*) 174.02(8), P(1)–Pt(1)–P(1*) 113.00(4), C(2)–Pt(1)–C(2*) 110.77(17).



Scheme 2

to establish the ligand dispositions and are similar in most cases to those of the corresponding adducts of **1**.³

In the dichloro complex **4**, the added chlorine atoms are mutually *trans*; no *cis*-dichloro isomer was formed, even after solutions of **4** in CH_2Cl_2 had been allowed to stand for several days at room temperature or solutions in toluene had been held at 100°C for 24 h. In contrast, the isolated di-iodo complex **6** has mutually *cis*-iodine atoms, one being *trans* to P and the other *trans* to C_{aryl} . No intermediate *trans* isomer was detected, unlike the corresponding reaction of iodine with **1**.³ The bromo complex **5** also appears to be mainly the *cis*-isomer but, as in the bromination of **1**,³ it was contaminated by a chelate phosphine oxide complex formulated as *cis*-[PtBr₂($\kappa^2\text{-C}_6\text{H}_3\text{-5-Me-2-PPh}_2$){ $\kappa^2\text{-O, C-C}_6\text{H}_3\text{-5-Me-2-P(O)Ph}_2$ }]}. Complex **7** contains mutually *trans*-iodo and -methyl groups; it appears not to isomerise rapidly to the *cis*-isomer, unlike the methyl iodide adduct of **1**.³

Treatment of **3** with one equivalent of PhICl_2 affords the *trans*-dichloro oxidative addition product [PtCl₂($\kappa^2\text{-C}_6\text{H}_3\text{-6-Me-2-PPh}_2$)], *trans*-**8** as a pale yellow solid. In contrast to **4**, however, this isomerises completely in CH_2Cl_2 over a period of hours to the corresponding *cis*-isomer (Scheme 2), presumably to relieve steric crowding of the 6-methyl groups in the *ortho*-metallated rings. The reaction of **3** with methyl iodide is far less clean than that of **2**, giving rise to numerous peaks in the regions δ 10–30 and 50–95 of the ³¹P NMR spectrum, perhaps indicative of disruption of the four-membered rings of **3**. However, the main identifiable product, formed in *ca.* 30% yield, appears to be the expected *trans*-(iodo)(methyl)platinum(IV) adduct **9**, which is accompanied by unchanged *cis*-**3** and its *trans*-isomer (see below).

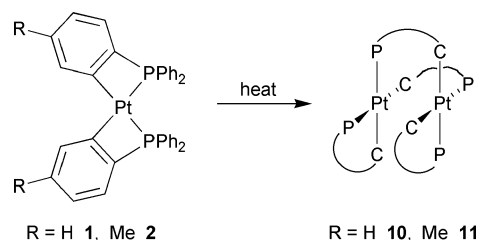
Thermolysis of the bis(chelate) complexes

When colourless solutions of **1** or **2** in toluene are heated under reflux for 24–48 h, their colour changes to yellow and dinuclear isomers of **1** or **2**, [Pt₂($\kappa^2\text{-C}_6\text{H}_3\text{-5-R-2-PPh}_2$)₂($\mu\text{-C}_6\text{H}_3\text{-5-R-2-PPh}_2$)₂] (R = H **10**, Me **11**) can be isolated in high yield (Scheme 3). Complex **11** shows a peak at m/z 1491 in the MALDI-mass spectrum corresponding to $[M + \text{H}]^+$ for the dimer. The ³¹P NMR spectra of **10** and **11** consist of two equally intense multiplets, with ¹⁹⁵Pt satellites, at *ca.* δ –60 and 25, suggestive of a pair of phosphorus atoms in two four-membered chelate rings and a pair in one eight-membered ring formed from bridging P–C ligands. Analysis of the spectra as an AA'MM'XX' spin system provided the coupling constants listed in Table 1. The magnitude of $J_{\text{P-P}}$ for the phosphorus atoms in the chelate rings (*ca.* 1200 Hz)

Table 1 ³¹P NMR parameters for [Pt₂($\kappa^2\text{-C}_6\text{H}_3\text{-n-R-2-PPh}_2$)₂($\mu\text{-C}_6\text{H}_3\text{-n-R-2-PPh}_2$)₂] (n = 5, R = H **10**, Me **11**; n = 6, R = Me **12**)^{a, b}

	10	11	12
$\delta(\text{P}_A)$	24.1	25.6	22.4
$\delta(\text{P}_B)$	–60.7	–60.0	–64.9
$J(\text{AX})$	2040	2030	2005
$J(\text{BX})$	1235	1219	1235
$J(\text{AA}')$	4	5	1
$J(\text{BB}')$	0	0	0
$J(\text{AX}')$	–150	–141	–122
$J(\text{BX}')$	0	0	0
$J(\text{AB})$	16	16	18
$J(\text{A}B')$	–10	–9	–9

^a Labelling of nuclei: B(A)X–X'(A')B', where $\text{P}_A, \text{P}_{A'}$ are the ³¹P nuclei of the bridging *ortho*-metallated ring, $\text{P}_B, \text{P}_{B'}$ are the ³¹P nuclei of the chelating *ortho*-metallated ring, and X = ¹⁹⁵Pt. $J(\text{XX}')$ could not be determined. ^b **10** and **11** in C_6D_6 , **12** in toluene.



Scheme 3

is even less than that in **1** or **2**, whereas $J_{\text{P-P}}$ for the phosphorus in the eight-membered rings (*ca.* 2030 Hz) is in the usual range (1800–2100 Hz) for P *trans* to $\sigma\text{-aryl}$.^{13,14}

The molecular structure of **10**, determined by single-crystal X-ray diffraction, is shown in Fig. 2 together with selected metrical data. It confirms the conclusions drawn from the spectroscopic data. Each platinum atom is in a distorted square planar environment formed by a pair of *cis*-phosphorus and *cis*-carbon atoms; one each of these atoms forms part of a four-membered chelate ring, the other two constitute with the two metal atoms a boat-shaped eight membered ring. The distance between the platinum atoms [3.3875(4) Å] is less than that in the structurally similar arsenic compound [Pt₂($\kappa^2\text{-C}_6\text{H}_3\text{-5-Me-2-AsPh}_2$)₂($\mu\text{-C}_6\text{H}_3\text{-5-Me-2-AsPh}_2$)₂][3.4208(3) Å]¹⁷ and may indicate a weak attractive interaction between the 5d⁸ metal centres.¹⁸ This small difference may also be due to other factors, for example, the smaller size of phosphorus compared to arsenic. The bite angle in the P–C–chelate ring [68.8(1)°] is similar to those in **1**–**3**. Although the Pt–C distances in the four- and eight-membered rings do not differ greatly [2.075(5), 2.060(5) Å, respectively], the Pt–P distance in the four-membered ring [2.321(1) Å] of **10** is significantly greater than that in the presumably less strained eight-membered ring [2.297(1) Å], thus reproducing the trend in the values of $J_{\text{P-P}}$. Surprisingly, it is also greater than the Pt–P distances in the four-membered rings of **1**–**3**.†

† A less precise structural determination of a different crystalline modification of **10** has been carried out at 296(2) K on a Philips PW 1100/20 diffractometer using Mo K α radiation.⁶² This form is monoclinic, space group $P2_1/a$, with a 25.380(2), b 19.842(2), c 14.050(2) Å, β 99.543(11)°, Z = 4. The molecular structure and metrical data are similar to those of the orthorhombic form, although the Pt...Pt separation is slightly less [3.361(1) Å].

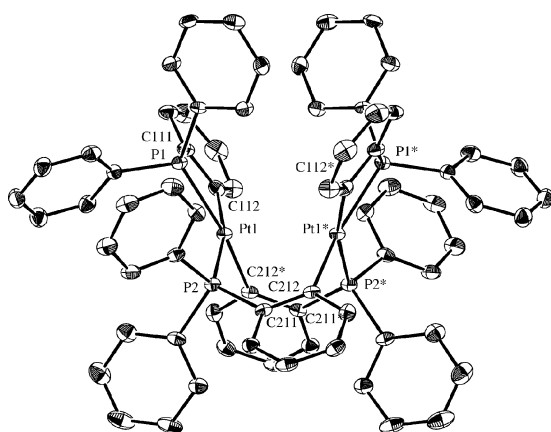


Fig. 2 Molecular structure of $[\text{Pt}_2(\kappa^2\text{-}2\text{-C}_6\text{H}_4\text{PPh}_2)_2(\mu\text{-}2\text{-C}_6\text{H}_4\text{PPh}_2)_2]$ **10**. Ellipsoids show 30% probability levels and hydrogen atoms have been deleted for clarity. Asterisks indicate atoms generated by crystallographic symmetry ($1 - x, \frac{3}{2} - y, z$). Selected bond lengths (Å) and angles ($^\circ$): Pt(1)–P(1) 2.321(1), Pt(1)–P(2) 2.297(1), Pt(1)–C(112) 2.070(5), Pt(1)–C(212*) 2.060(5), Pt(1)⋯Pt(1*) 3.3875(4), P(1)–Pt(1)–P(2) 103.71(5), P(1)–Pt(1)–C(112) 68.8(1), P(1)–Pt(1)–C(212*) 157.7(1), P(2)–Pt(1)–C(112) 166.4(2), P(2)–Pt(1)–C(212*) 92.7(1), C(112)–Pt(1)–C(212*) 91.8(2).

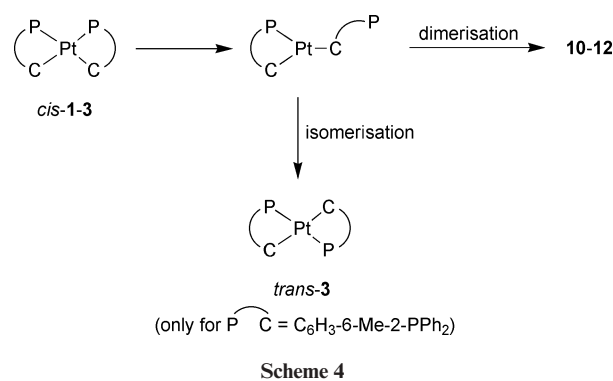
Attempts to open the remaining chelate rings of **10** or **11** to form a lantern-type dimer in which all four *ortho*-metallated ligands bridge the two platinum atoms were unsuccessful. Complex **11** was recovered unchanged, with only a trace of decomposition, even after 2 weeks in refluxing mesitylene or after UV-irradiation for several hours. That a lantern structure can be generated by heating the arsenic analogue of **11**¹⁷ may be attributed to the weaker Pt–As bonds, which allow facile dissociation and binding to the neighbouring metal atom.

Heating a suspension of the 6-methyl compound *cis*-**3** in toluene gave only traces of the corresponding dimer **12**, which was identified by the appearance of two, equally intense multiplets in the ³¹P NMR spectrum at δ –64.9 and 22.4; the derived coupling constants are similar to those in **10** and **11** (Table 1). The main product was *trans*- $[\text{Pt}(\kappa^2\text{-C}_6\text{H}_3\text{-}6\text{-Me-}2\text{-PPh}_2)_2]$, *trans*-**3**, which was isolated as a poorly soluble, white solid in 62% yield. Its EI-mass spectrum contains a parent ion peak at m/z 745, and the ³¹P NMR spectrum shows a singlet at δ –62.9 (J_{PtP} 2445 Hz). The chemical shift confirms that the four-membered rings have been retained and the coupling constant is typical of P *trans* to P in planar Pt(II) complexes.¹⁹

We assume that the dimers **10** and **11** are formed by initial dissociation of the phosphorus end of one of the chelate rings of *cis*-**1** or *cis*-**2** and subsequent recombination of the two three-coordinate fragments (Scheme 4). For *cis*-**3**, the first step is the same, but the presence of the sterically hindering 6-methyl group presumably favours *cis* → *trans* isomerisation over dimerisation.

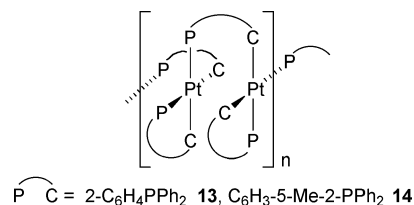
Reactions with carbon monoxide

Exposure of solutions of **1** or **2** to CO (1–2 bar) at room temperature causes an immediate colour change to yellow and the formation of a white precipitate. From the solution, the dinuclear complexes **10** or **11** can be isolated in *ca.* 40% yield; evidently CO catalyses opening of one of the four-membered chelate rings of **1**



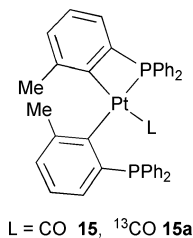
or **2** at room temperature. The colourless solids, **13** and **14**, which are formed in comparable amounts to **10** or **11**, are insoluble in common organic solvents. Unexpectedly, their IR spectra show no bands in the region 2000–2100 cm^{-1} or 1700–1850 cm^{-1} typical of terminal or acyl C–O stretching, respectively. Elemental analyses were somewhat variable and suggest that a small amount of Cl, presumably arising from CH_2Cl_2 that had been used in work-up, was present. The composition of **14** seemed to correspond approximately to the formula $[\text{Pt}(\text{C}_6\text{H}_3\text{-}5\text{-Me-}2\text{-PPh}_2)_2]$. That **13** and **14** are indeed isomers of **10** and **11**, respectively, is indicated by the observation that they are converted into **10** or **11** on heating in toluene for 24 h.

The solid state ³¹P NMR spectrum of **14** consists of two resonances of about the same intensity at δ –61.0 and 19.0, each flanked by ¹⁹⁵Pt satellites (J_{PtP} 1118 Hz and 2119 Hz, respectively). The chemical shifts and coupling constants are similar to those of **10** and **11**, which suggests that the disposition of ligand atoms in **14** is similar to that in **10** and **11**. On this basis we assign **13** and **14** the structures shown, in which the bridging $\text{C}_6\text{H}_3\text{-}5\text{-R-}2\text{-PPh}_2$ (R = H, Me) groups span platinum atoms in neighbouring units, thus making an infinite chain polymer and accounting for the poor solubility in organic solvents.

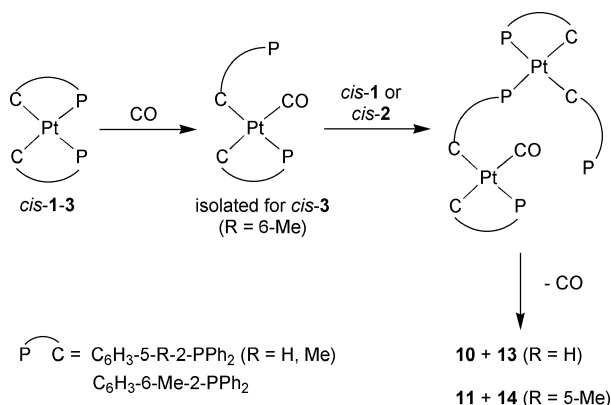


Complex *cis*-**3** also reacts readily with CO at room temperature and pressure but the product in this case is a mono-carbonyl complex $[\text{Pt}(\text{CO})(\kappa\text{C-C}_6\text{H}_3\text{-}6\text{-Me-}2\text{-PPh}_2)(\kappa^2\text{-C}_6\text{H}_3\text{-}6\text{-Me-}2\text{-PPh}_2)]$ **15**, which can be isolated in quantitative yield. The added CO is lost slowly from the solid at room temperature, and more rapidly *in vacuo* over a period of 24 h, to give *trans*-**3**, hence satisfactory elemental analyses were not obtained. The structure can be assigned unequivocally on the basis of spectroscopic data. There is a parent-ion peak at m/z 773 in the EI-mass spectrum and a strong $\nu(\text{CO})$ band at 2053 cm^{-1} in the IR spectrum, *cf.* 2050 cm^{-1} for *cis*- $[\text{PtPh}_2(\text{CO})(\text{PPh}_3)]$ and 2048 cm^{-1} for *cis*- $[\text{PtPh}_2(\text{CO})(\text{PMePh}_2)]$.²⁰ The ³¹P NMR spectrum consists of a pair of doublets at δ –12.3 and –62.4 (J_{PP} 2.2 Hz), each with Pt satellites (J_{PtP} 179 Hz and 1130 Hz, respectively). The chemical shift and small J_{PtP} for the first resonance are characteristic of uncoordinated phosphorus in this type of compound, *cf.* $[\text{Pt}(\text{L})(\kappa\text{C-}2\text{-C}_6\text{H}_4\text{PPh}_2)(\kappa^2\text{-}2\text{-C}_6\text{H}_4\text{PPh}_2)]$

[L = PPh₃, P(OPh)₃, P(OMe)₃, Bu^tNC];³ the second resonance clearly belongs to bidentate κ²-C₆H₃-6-Me-2-PPh₂. The similarly prepared ¹³C O adduct **15a** shows a pair of bands due to ν(CO) in its IR spectrum at 2004 and 1996 cm⁻¹ (presumably a solid state splitting); the ³¹P NMR spectrum displays a doublet at δ -12.5 (unresolved *J*_{PP}/*J*_{PC} 1.9 Hz, *J*_{PtP} 179 Hz) and a doublet of doublets at -62.5 (*J*_{PP} 2.3 Hz, *J*_{PC} 3.6 Hz, *J*_{PtP} 1129 Hz). The ¹³C NMR spectrum also contains a doublet of doublets at δ 176.6 (*J*_{PC} 1.4, 3.6 Hz) due to ¹³C O flanked by ¹⁹⁵Pt satellites (*J*_{PtC} 1102 Hz). The small values of *J*_{PtC} and *J*_{PC} are consistent only with a structure for **15** in which CO is *trans* to the aryl carbon of the bidentate P-C ligand.²¹⁻²³



These observations indicate that coordination of CO to platinum, triggering dissociation of the phosphorus end of one of the chelate ligands, is a plausible first step in the CO-catalysed dimerisation and polymerisation of **1** and **2**, as shown in Scheme 5. The dangling phosphine can then coordinate to another platinum centre, thus initiating dimerisation or polymerisation, with elimination of CO. In the reaction of *cis*-**3** with CO, complex **15**, which models the intermediate carbonyl complex proposed in the cases of *cis*-**1** and *cis*-**2**, can be isolated, probably because the 6-methyl groups block any intermolecular coordination of the displaced phosphorus atom. It may seem surprising at first sight that CO does not insert in the Pt-C σ-bond in the first step, since this would lead to a presumably less strained, five-membered chelate acyl containing the ligand κ²-P,C-COC₆H₃-5-R-2-PPh₂ (R = H, Me). This type of reaction occurs readily for *ortho*-metallated PPh₃ complexes of Mn(I),²⁴ Ru(II),²⁵ Co(I)²⁶ and Rh(I).²⁷ In the first step, however, CO is presumably located *trans* to the aryl carbon atom of the bidentate P-C ligand, as found for **15**, and therefore cannot undergo *cis*-insertion into the aryl carbon-metal bond of the four-membered ring.²³



Scheme 5

Formation and reactions of diplatinum(I) complexes

Comproportionation of **1** or **2** with [Pt(PPh₃)₃] or [Pt(PPh₃)₂(C₂H₅)] in refluxing toluene gives, in 75–80% isolated yield, bright yellow, microcrystalline diplatinum(I) complexes [Pt₂(μ-C₆H₃-5-R-2-PPh₂)₂(PPh₃)₂] (R = H **16**, Me **17**) derived by opening of the four-membered rings in **1** or **2**. The X-ray structure and ³¹P NMR spectrum of **16** were reported in a preliminary communication,² and a more precise structural determination of **17** is described below.

Attempted reaction of *cis*-**3** with [Pt(PPh₃)₃] gave a complex mixture and no 6-methyl analogue of **16** or **17** could be identified in the ³¹P NMR spectrum. Attempts to generate a Pt-Pd analogue of **17** by use of [Pd(PPh₃)₄] in place of [Pt(PPh₃)₃] also failed.

The MALDI-mass spectrum of **17** contains a peak at *m/z* 1465 corresponding to the [M + H]⁺ fragment and the ¹H NMR spectrum shows a single methyl resonance, indicating that the bridging groups are in identical environments. The ³¹P NMR spectrum consists of two 1 : 2 : 1 triplets (AA'BB' pattern) centred at δ -3.0 and 26.3 due to μ-C₆H₃-5-Me-2-PPh₂ (P_A) and coordinated PPh₃ (P_B), respectively. Satellites arising from isotopomers containing one and two ¹⁹⁵Pt nuclei are also present. The spectrum can be simulated to provide the P-P and Pt-P coupling constants that are listed in Table 2, together with those previously reported for **16**.² The parameters are similar both to each other and to those of the structurally similar compound derived from 1,2-bis(diphenylphosphino)ethane (dppe), *viz.*, [Pt₂{μ-C₆H₄P(Ph)CH₂CH₂PPh₂}₂].²⁸ There is a minor difference in the magnitude of *J*_{PtP} for the phosphorus atom of the *ortho*-metallated ring (1937 Hz for **16**, 1918 Hz for **17**), which can be attributed to the electronic effect of the *p*-methyl substituent. The magnitude of *J*_{PtP} for P *trans* to C (1866 Hz) and P *trans* to Pt-Pt (1862 Hz) indicate that the Pt-Pt bond has a similar *trans*-influence to that of Pt-C(aryl).

The molecular structure of **17** determined by single-crystal X-ray diffraction analysis is shown in Fig. 3, together with significant metrical data. A pair of platinum atoms is coordinated by two bridging C₆H₃-5-Me-2-PPh₂ groups and two axial PPh₃ ligands, each platinum atom being in a distorted square planar coordination environment. The Ph₃P-Pt-Pt-PPh₃ unit is close

Table 2 ³¹P NMR parameters for [Pt₂(μ-C₆H₃-5-R-2-PPh₂)(PPh₃)₂] (R = H **16**, Me **17**) and [Pt₂(μ-Y)(μ-C₆H₃-5-R-2-PPh₂)(PPh₃)₂]⁺ (Y = I, R = H [**19**]⁺, Me [**20**]⁺; Y = H, R = H [**22**]⁺)^{a,b}

	16	17	[19] ⁺	[20] ⁺	[22] ⁺
δ(P _A)	-3.6	-3.0	5.6	5.0	3.1
δ(P _B)	24.1	26.3	15.5	16.1	22.9
<i>J</i> (AX)	1937	1918	1677	1674	1704
<i>J</i> (BX)	1866	1862	5065	5080	3701
<i>J</i> (AA')	±55	56	29	30	48
<i>J</i> (BB')	±226	228	0	0	66
<i>J</i> (AX')	-140	-140	0	0	-50
<i>J</i> (BX')	1149	1160	123	123	387
<i>J</i> (AB)	10	11	20	20	18
<i>J</i> (AB')	10	11	0	0	0

^a Labelling of nuclei: B(A)X-X'(A')B', where P_A, P_{A'} are the ³¹P nuclei in the bridging *ortho*-metallated ring, P_B, P_{B'} are the ³¹P nuclei of the PPh₃ ligands, and X = ¹⁹⁵Pt. Note that the labelling of X, X' is reversed from that used in ref. 2. *J*(XX') could not be determined. ^b **16** and **17** measured in C₆D₆, **19**, **20** and **22** in CD₂Cl₂.

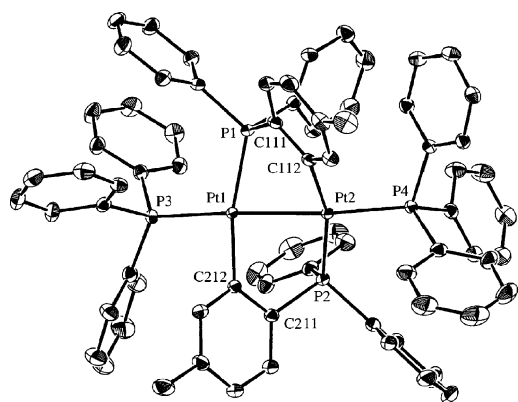
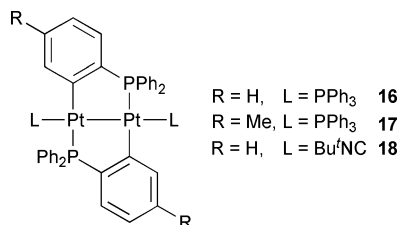


Fig. 3 Molecular structure of $[\text{Pt}_2(\mu\text{-C}_6\text{H}_3\text{-5-Me-2-PPh}_2)_2(\text{PPh}_3)_2]$ **17**. Ellipsoids show 30% probability levels and hydrogen atoms have been deleted for clarity. Selected bond lengths (\AA) and angles ($^\circ$): Pt(1)–Pt(2) 2.61762(16), Pt(1)–P(1) 2.3014(8), Pt(1)–P(3) 2.29505(8), Pt(1)–C(212) 2.045(3), P(1)–Pt(1)–C(212) 163.39(9), Pt(2)–Pt(1)–P(3) 173.12(2), P(1)–Pt(1)–P(3) 102.73(3), Pt(2)–Pt(1)–C(212) 85.61(8).

to linear. The Pt–Pt distance [2.61762(16) \AA] is similar to that of **16** [2.630(1) \AA]² and $[\text{Pt}_2\{\mu\text{-C}_6\text{H}_4\text{P(Ph)CH}_2\text{CH}_2\text{PPh}_2\}_2]$ [2.628(1) \AA],²⁸ and is consistent with the presence of a direct Pt(1)–Pt(1) ($5d^9\text{-}5d^9$) bond. The similar Pt–P bond lengths for $\mu\text{-C}_6\text{H}_3\text{-5-Me-2-PPh}_2$ [2.3014(8) \AA] and PPh_3 [2.2905(8) \AA] can be compared with that found in *cis*- $[\text{PtCl}_2(\text{PPh}_3)_2]$ [2.264(7) \AA];²⁹ they reflect the high *trans*-influence of the Pt–C(aryl) and Pt–Pt bonds inferred from the ^{31}P NMR data.

In light of the chemistry already described, it seems plausible that **16** and **17** are formed by coordination of dangling phosphorus atoms arising from opening of the four-membered rings of **1** and **2** to a $\text{Pt}(\text{PPh}_3)_2$ fragment generated by dissociation of **L** from $[\text{Pt}(\text{PPh}_3)_2(\text{L})]$ ($\text{L} = \text{PPh}_3, \text{C}_2\text{H}_4$).

The axial PPh_3 ligands of **16** are replaced rapidly by *t*-butyl isocyanide at room temperature to give the diplatinum(II) complex $[\text{Pt}_2(\mu\text{-2-C}_6\text{H}_4\text{PPh}_2)_2(\text{CNBu}^t)_2]$ **18** as a pale yellow solid. It shows a $\nu(\text{C}\equiv\text{N})$ band at 2125 cm^{-1} in the IR spectrum and resonances typical of Bu^tNC in its ^1H and ^{13}C NMR spectra. The ^{31}P NMR spectrum contains only a singlet in the region of $\delta -4$ due to equivalent $2\text{-C}_6\text{H}_4\text{PPh}_2$ ligands accompanied by satellite peaks due to the mono- ^{195}Pt and bis- ^{195}Pt isotopomers. Analysis of the AA'X and AA'XX' sub-spectra³⁰ yields the parameters shown in Table 3; the derived value of 4421 Hz for $^1J_{\text{PtPt}}$ suggests that a metal–metal bond is present, although there is a wide variation in the magnitude of this coupling constant even in compounds that are known to contain Pt–Pt bonds.^{30–32}



Carbon monoxide also displaces PPh_3 from **16** at room temperature but the products are stable in solution only under CO. The first-formed compound, which precipitates to some extent when the reaction is done in hexane, shows a strong $\nu(\text{CO})$ band at

Table 3 ^{31}P NMR parameters for $[\text{Pt}_2(\mu\text{-2-C}_6\text{H}_4\text{PPh}_2)_2(\text{CNBu}^t)_2]$ **18** and $[\text{Pt}_2(\mu\text{-H})(\mu\text{-2-C}_6\text{H}_4\text{PPh}_2)(\text{CNBu}^t)_2]^+$ **21**^a

	18	21 ⁺
δ	−4.2 ^b	6.2 ^c
$J(\text{AX})$	1920	1514
$J(\text{AA}')$	64	58
$J(\text{AX}')$	−137	−74
$J(\text{XX}')$	4421	2711

^a Labelling of nuclei: $\text{AX}\cdots\text{A}'\text{X}'$, where A, A' are the ^{31}P nuclei in the bridging *ortho*-metallated ring and X = ^{195}Pt . ^b In C_6D_6 . ^c In CD_2Cl_2 .

2022 cm^{-1} and is probably the mono-carbonyl. In other solvents products having more complex spectra are obtained, which have not been investigated further.

Treatment of complexes **16** and **17** with one equivalent of iodine in CH_2Cl_2 gives the orange, A-frame diplatinum(II) complexes $[\text{Pt}_2(\mu\text{-I})(\mu\text{-C}_6\text{H}_3\text{-R-2-PPh}_2)_2(\text{PPh}_3)_2]\text{I}$ ($\text{R} = \text{H}$ [**19**]I; $\text{R} = \text{Me}$ [**20**]I). The X-ray structure and NMR data for [**19**]I were reported previously.² The MALDI-mass spectrum of [**20**]⁺ shows the expected $[\text{M} + \text{H}]^+$ peak at m/z 1592 and the ^1H NMR spectrum shows a single methyl resonance at δ 1.53, confirming that the bridging $\text{C}_6\text{H}_3\text{-5-Me-2-PPh}_2$ groups are in equivalent environments. The ^{31}P NMR spectrum of [**20**]⁺, like that of [**19**]⁺, shows two main resonances, as approximately 1 : 1 : 1 : 1 quartets, at δ 5.0 and 16.1, for the $\mu\text{-C}_6\text{H}_3\text{-5-Me-2-PPh}_2$ (P_A) and PPh_3 (P_B) ligands, respectively, with sub-spectra arising from P–P and Pt–P coupling. The derived coupling constants are listed in Table 2. Disruption of the Pt–Pt interaction in **16** and **17** by iodine is indicated by the reduction of the P–P coupling between the PPh_3 ligands from *ca.* 230 Hz to zero, and by the reduction of the indirect Pt– PPh_3 coupling ($J_{\text{BX}'}$) from 1160 Hz to 123 Hz. The large increase in the direct coupling (J_{BX}) from *ca.* 1870 Hz in **16** and **17** to more than 5000 Hz in [**19**]⁺ and [**20**]⁺ is consistent with P *trans* to halide; the remarkably high value appears also to be characteristic of halide *cis* to an aryl or aroyl group in binuclear platinum(II) complexes.³³

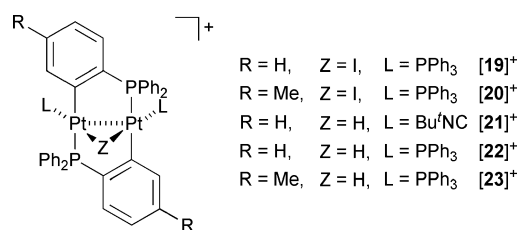
Treatment of complex **16** with an excess of HCl cleaves both the Pt–Pt and Pt–C bonds giving *cis*- $[\text{PtCl}_2(\text{PPh}_3)_2]$, but strong acids containing poorly coordinating anions react with **16–18** forming μ -hydridodiplatinum(II) cations having an A-frame structure, which are readily identified by ^1H and ^{31}P NMR spectroscopy. Thus, complex **18** reacts with HBF_4 to give the colourless salt $[\text{Pt}_2(\mu\text{-H})(\mu\text{-2-C}_6\text{H}_4\text{PPh}_2)_2(\text{CNBu}^t)_2]\text{BF}_4$ [**21**] BF_4 , whose hydride resonance appears at $\delta -8.7$ as the expected 1 : 8 : 18 : 8 : 1 quintet of triplets arising from coupling with a pair of equivalent platinum atoms and a pair of phosphorus nuclei (J_{PtH} 760 Hz, J_{PH} 7 Hz). The Pt–Pt coupling constant derived from the ^{31}P NMR spectrum of [**21**]⁺, *ca.* 2700 Hz, is less than that in its precursor **18** (Table 3), consistent with a weakening of the Pt–Pt bond by protonation. Complex **16** is protonated similarly by HBF_4 , HPF_6 , $\text{CF}_3\text{CO}_2\text{H}$, $\text{CF}_3\text{SO}_3\text{H}$ or *p*- tolSO_3H to give colourless salts of the cation $[\text{Pt}_2(\mu\text{-H})(\mu\text{-2-C}_6\text{H}_4\text{PPh}_2)_2(\text{PPh}_3)_2]^+$ [**22**]⁺. The ^1H NMR spectrum of the cation shows a hydride resonance at $\delta -5.17$ in which the inner three resonances of the 1 : 8 : 18 : 8 : 1 quintet of triplets are split further into 1 : 2 : 1 triplets owing to strong coupling with the ^{31}P nuclei of the two PPh_3 ligands that are *trans* to hydride (J_{PH} 80 Hz); the outer resonances were not detected. The chemical shift and Pt–H coupling constant (735 Hz) are similar to those observed for

the bridging hydride in $[\text{Pt}_2\text{H}_2(\mu\text{-H})(\mu\text{-dppm})_2]\text{PF}_6$ ($\delta -5.86$, J_{PtH} 540 Hz).³⁴ No band assignable to $\nu(\text{PtH})$ could be detected in the IR spectra of $[\mathbf{21}]^+$ or $[\mathbf{22}]^+$.

The Pt–P and P–P coupling constants derived from analysis of the ^{31}P NMR spectrum of $[\mathbf{22}]^+$ are given in Table 2. Notable is the magnitude of J_{PIP} , 3701 Hz, to the phosphorus atoms of the PPh_3 ligands, which are *trans* to the bridging hydride in an ideal A-frame structure, *cf.* the unexpectedly large values of the same coupling constants *trans* to bridging iodide in $[\mathbf{19}]^+$ and $[\mathbf{20}]^+$ (see above). In mononuclear Pt(II) complexes a J_{PIP} value of 3701 Hz would imply that the phosphorus atom was *trans* to a strongly electron-withdrawing or weakly bonded ligand.¹⁹ A similar observation has been made in the case of the $(\mu\text{-hydrido})(\mu\text{-diphenylphosphido})\text{diplatinum(II)}$ cation $[(\text{PPh}_3)(\text{Ph})\text{Pt}(\mu\text{-H})(\mu\text{-PPh}_2)\text{Pt}(\text{PPh}_3)_2]^+$, for which $J_{\text{PIP}}(\text{PPh}_3)$ *trans* to hydride is 3785 Hz.^{35,36} The relatively low *trans*-influence of bridging hydride has been noted in other dinuclear platinum(II) complexes.^{34–37}

Treatment of $[\mathbf{22}]^+$ with aqueous K_2CO_3 at 40 °C or NH_3 at room temperature re-forms **16** quantitatively. The reaction with Bu^nLi is more complicated. Only *ca.* half the expected quantity of **16** is formed, together with approximately equal amounts of two other compounds that have not been separated or identified.

The corresponding salt $[\text{Pt}_2(\mu\text{-H})(\mu\text{-C}_6\text{H}_3\text{-5-Me-2-PPh}_2)_2(\text{PPh}_3)_2]\text{PF}_6$ $[\mathbf{23}]\text{PF}_6$ obtained from **17** and HPF_6 shows a peak in its MALDI-mass spectrum at m/z 1465 corresponding to $[M - \text{PF}_6]^+$ and a hydride resonance at $\delta -5.22$ (J_{PtH} 735 Hz) in the ^1H NMR spectrum similar in multiplicity to that of $[\mathbf{22}]^+$, though less well resolved. Unexpectedly, however, there are three aromatic methyl resonances of equal intensity, suggesting that $[\mathbf{23}]\text{PF}_6$ may not be a single compound. The ^{31}P NMR spectrum resembles that of $[\mathbf{22}]^+$ in its general features: there are two multiplets of equal intensity at *ca.* δ 23.5 and 3 due to PPh_3 and the *ortho*-metallated ligand, respectively, the former showing two pairs of ^{195}Pt satellites (J_{PIP} *ca.* 3900, 400 Hz) and the latter one pair (J_{PIP} *ca.* 1700 Hz). However, the spectrum of $[\mathbf{23}]^+$ is more complex than that of $[\mathbf{22}]^+$ and simulation was not attempted.



The X-ray structure of the cation in $[\mathbf{23}]\text{PF}_6$ is shown in Fig. 4; selected bond lengths and angles are collected in Table 4. The geometry of the cation is similar to that of the μ -iodo cation in $[\mathbf{19}]\text{I}$. The hydride ligand H(1), which was located in the difference electron-density map, occupies the apical position. The cation is disordered in such a way that the phosphine ligand containing P(1) is *ortho*-metallated to Pt(2) to the extent of 75% *via* the *p*-tolyl group and 25% *via* a P–Ph group of the bridging unit. Correspondingly, the phosphine ligand containing P(2) is *ortho*-metallated to Pt(1) to the extent of 30% *via* the *p*-tolyl group and 70% *via* a P–Ph group. This scrambling of *p*-methyl groups between the aryl groups of the *ortho*-metallated unit accounts for the appearance of several ^1H aromatic methyl resonances in solution arising from closely related, isomeric species.

Table 4 Selected bond distances (Å) and angles (°) in $[\text{Pt}_2(\mu\text{-H})(\mu\text{-C}_6\text{H}_3\text{-5-Me-2-PPh}_2)_2(\text{PPh}_3)_2]\text{PF}_6 \cdot \text{H}_2\text{O} \cdot 0.48\text{Et}_2\text{O}$ $[\mathbf{23}]\text{PF}_6$

Pt(1)–P(1)	2.3424(14)	Pt(1)–P(3)	2.3099(15)
Pt(2)–P(2)	2.3602(13)	Pt(2)–P(4)	2.2958(13)
Pt(1)–C(212)	2.071(5)	Pt(2)–C(112)	2.082(4)
Pt(1)···Pt(2)	2.7888(3)	Pt(1)–H(1)	1.62(1)
Pt(2)–Pt(1)–P(3)	161.32(4)	Pt(1)–Pt(2)–P(4)	164.64(3)
P(1)–Pt(1)–P(3)	100.52(5)	P(2)–Pt(2)–P(4)	101.04(5)
Pt(2)–Pt(1)–C(212)	91.03(14)	Pt(1)–Pt(2)–C(112)	91.89(14)
Pt(1)–Pt(2)–P(2)	77.06(3)	Pt(2)–Pt(1)–H(1)	30.5(4)
Pt(1)–Pt(2)–H(1)	30.4(4)		

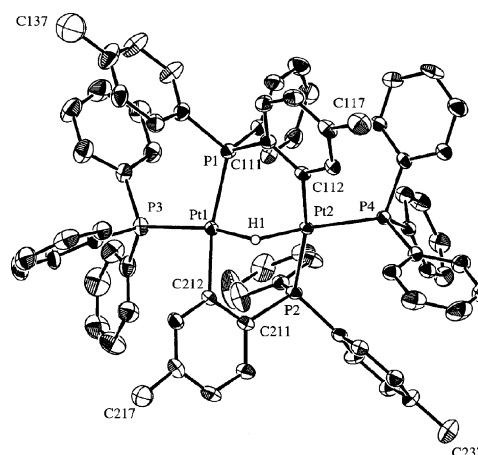
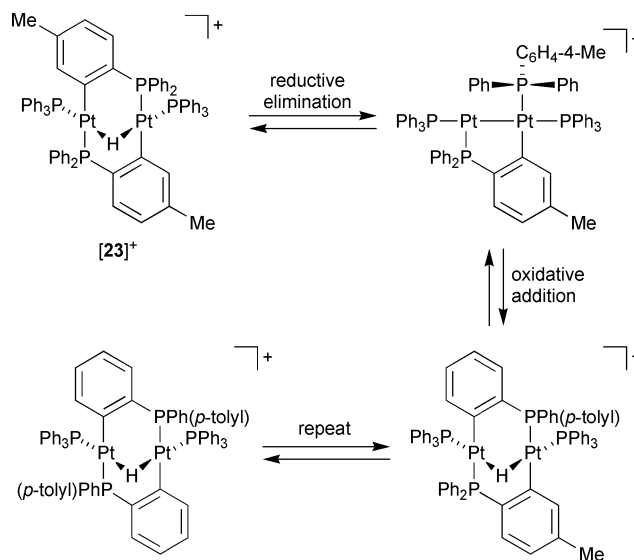


Fig. 4 Molecular structure of the cation of $[\text{Pt}_2(\mu\text{-H})(\mu\text{-C}_6\text{H}_3\text{-5-Me-2-PPh}_2)_2(\text{PPh}_3)_2]\text{PF}_6 \cdot \text{H}_2\text{O} \cdot 0.48\text{Et}_2\text{O}$ $[\mathbf{23}]\text{PF}_6$. Ellipsoids show 30% probability levels. Hydrogen atoms, with the exception of the bridging hydride, have been deleted for clarity.

The process responsible for the scrambling is probably reversible C–H reductive elimination and oxidative addition, as shown in Scheme 6. The μ -hydride in $[\mathbf{23}]^+$ can undergo reductive elimination with one of the bridging *p*-tolyl groups forming coordinated 4-tolyl-diphenylphosphine, and leaving one bridging *ortho*-metallated group. The reverse process of C–H oxidative addition that regenerates μ -hydride can then occur either from



Scheme 6

a 4-tolyl or a phenyl group of 4-tolylidiphenylphosphine, giving, in the latter case, bridging 2-C₆H₄P(Ph)(C₆H₄-*p*-Me). The process can be repeated with the second bridging C₆H₃-5-Me-2-PPh₂ ligand. Reductive elimination of benzene and alkanes, respectively, from mononuclear *cis*-hydrido(phenyl)- and *cis*-hydrido(alkyl)-platinum(II) complexes, *cis*-[PtH(R)(PPh₃)₂], occurs readily, but, in contrast with the behaviour reported here, these processes are irreversible.³⁸

The Pt–Pt separation in [23]PF₆ [2.7888(3) Å] is greater than that in 17 [2.61762(16) Å], demonstrating the expected lengthening, and presumably weakening, of the metal–metal bond in the latter on protonation. The corresponding separation in the μ-iodo cation [19]⁺, 2.931(2) Å, is even greater, probably because of the larger bridging ligand. The Pt–Pt separation in [23]PF₆ is also significantly less than in mono-μ-hydrido complexes, such as *trans*-YL₂Pt(μ-H)PtY'L₂⁺ (Y = Y' = H, L = PEt₃; Y = H, Y' = Ph, L = PEt₃; Y = Y' = Ph, L = PMe₃, PEt₃; Y = Y' = C₆F₅, L = PMe₃), whose Pt–Pt distances are in the range 3.00–3.25 Å.^{39–42} However, mono-μ-hydridodiplatinum(II) complexes that contain another bridging group, such as μ-PPh₂, μ-S or μ-C≡CR, or complexes that have *cis*-bidentate instead of *trans*-tertiary phosphines, have Pt–Pt separations that are similar to that in [23]PF₆, e.g., [Pt₂(μ-H)(μ-CO)(dppe)₂]BF₄ [2.716(1) Å],⁴³ [Pt₂(μ-H)(μ-S)(dppe)₂]BF₄ [2.774(1) Å],⁴⁴ [(Ph)(Ph₃P)Pt(μ-H)(μ-PPh₂)Pt(PPh₃)₂]Y [Y = BF₄, 2.889(2), 2.912(2) Å, independent molecules; Y = CH(SO₂CF₃)₂, 2.885(1) Å],^{35,36} [Pt₂(μ-H)(μ-C≡CPh)(C₆F₅)₂(PPh₃)₂] [2.8159(10) Å],⁴⁵ and [Pt₂H₂(μ-H)(L–L)]BF₄ [L–L = EtN(PPh₂)CHEtCH₂OPPh₂, 2.736(1) Å].⁴⁶ Thus, the three-centre Pt–H–Pt interaction in [23]PF₆ appears to be “closed” and to retain some Pt–Pt bonding. The Pt–H distances, which were restrained to be equal in the positional refinement, were found to be 1.62(1) Å and the angle subtended at the hydride about 119(1)°. These parameters are comparable with those cited for other mono-μ-hydridodiplatinum(II) complexes, e.g. *trans*-[R(Me₃P)₂Pt(μ-H)PtR(PMe₃)₂]BPh₄ [1.79(8), 1.73(7) Å, 121(5)° for R = Ph; 1.6(1), 1.7(1) Å, 126(9)° for R = C₆F₅].⁴² The P(3)–Pt(1)–Pt(2) and P(4)–Pt(2)–Pt(1) angles [161.32(4)° and 164.64(3)°, respectively] are smaller than those observed in 17 owing to the presence of the bridging hydride.

The Pt–P distances to the *ortho*-metallated ligands of [23]PF₆ [2.3424(14), 2.3602(13) Å] are significantly greater than those in 17 [2.3014(8), 2.3030(8) Å], reflecting the trend in Pt–P coupling constants of 17 and [22]⁺ (Table 2). On the other hand, the Pt–PPh₃ distances in 17 and [23]PF₆ are unexceptional (*ca.* 2.30 Å) and do not differ significantly, even though the magnitude of *J*_{PtP}(PPh₃) (3701 Hz) in the latter is about twice that in the former (see above and Table 2). This situation differs from that in [Ph(Ph₃P)Pt(μ-H)(μ-PPh₂)Pt(PPh₃)₂]⁺, in which the Pt–P(PPh₃) distance *trans* to the bridging hydride is significantly shorter [2.270(8) Å,³⁵ 2.274(3) Å³⁶] than the other Pt–P(PPh₃) distances (2.32–2.33 Å), corresponding to the unexpectedly large Pt–P coupling constant (3785 Hz). Venanzi *et al.*³⁵ suggested that this might indicate the hydride in the μ-PPh₂ cation (which was not located directly) to be bridging unsymmetrically between the two platinum atoms, but this clearly cannot apply to [23]PF₆. Perhaps the simplest explanation for the large Pt–P coupling constant *trans* to μ-hydride in [23]⁺ is that the high demand for Pt 6s-electron density made by hydride can be shared equally between the two platinum atoms, hence the Pt–P coupling constant, which reflects this demand,⁴⁷

is about twice its value in mononuclear Pt(II) hydrides having hydride *trans* to PR₃ (e.g. 1984 Hz in *cis*-[PtH₂(PEt₃)₂]).⁴⁸ A similar explanation has been advanced to account for the magnitude of *J*_{PtP} (2741 Hz) in the *cis*-[PtH₂(PEt₃)₂] moiety of *cis*-[(Et₃P)₂Pt(μ-H)₂PtH(PEt₃)₂]⁺.³⁷

Conclusions

The bis(chelate) complexes *cis*-[Pt(κ²-C₆H₃-5-R-2-PPh₂)₂] (R = H 1, Me 2) are not thermodynamically stable and are converted on heating, or on treatment with CO, into dimers containing bridging and chelating ligands, [Pt₂(κ²-C₆H₃-5-R-2-PPh₂)₂(μ-C₆H₃-5-R-2-PPh₂)₂] (R = H 10, Me 11). In contrast with the analogous tertiary arsine system, these dimers do not isomerise further to complexes containing four bridging carbanionic ligands. Dimer formation probably proceeds by initial dissociation of the phosphorus end of the chelate ring. The presence of a 6-methyl substituent sterically inhibits dimer formation, so that *cis*-[Pt(κ²-C₆H₃-6-Me-2-PPh₂)₂], *cis*-3, preferentially isomerises to *trans*-3 on heating, and reacts with CO to give a platinum(II) carbonyl complex 15 containing C₆H₃-6-Me-2-PPh₂ behaving unusually as a monodentate, C-bonded ligand. Likewise, comproportionation of 1 and 2 with [Pt(PPh₃)₂L] (L = PPh₃, C₂H₄) to give the metal–metal bonded, diplatinum(I) complexes 16 and 17 occurs cleanly for 2-C₆H₄PPh₂ and C₆H₃-5-Me-2-PPh₂, whereas the attempted formation of a diplatinum(I) complex from 3 by a similar route failed. Although the 5-methyl substituent in the carbanion makes little difference to the chemistry of platinum(II) and diplatinum(I), its presence helps to establish the occurrence of a reversible reductive elimination–oxidative addition sequence between hydride and the metal–aryl bonds of the bridging carbanion in [23]⁺. Reductive elimination and oxidative addition reactions involving hydride and methyl ligands are a well-established feature of the diplatinum(I) chemistry of μ-bis(diphenylphosphino)methane and related ligands.⁴⁹

Experimental

All experiments were carried out in an inert atmosphere with use of standard Schlenk techniques, though the platinum complexes were stable to air once isolated. Solvents were dried and degassed by standard procedures. Triflic acid was distilled before use; all other materials were used without further purification. The NMR spectra were measured on Jeol FX 200 (¹³C 50.3 MHz, ³¹P 81.0 MHz), Varian Gemini 2000 (¹³C 50.3 MHz), Varian XL-200 (³¹P 81.0 MHz) and Bruker Aspect 2000 (¹H 300 MHz, ³¹P 121.0 MHz) instruments. The ¹H and ¹³C chemical shifts (δ) were measured relative to the residual signals of CD₂Cl₂ (δ_H 5.32, δ_C 52.6), C₆D₆ (δ_H 7.15, δ_C 128.0) or CDCl₃ (δ_H 7.26, δ_C 77.0); ³¹P NMR spectra were recorded with 85% H₃PO₄ as external reference. Spectral simulations were carried out on an in-house program at the University of Victoria, British Columbia, Canada or by use of the gNMR program.⁵⁰ Infrared spectra were measured as KBr discs on Perkin Elmer 683 grating, Spectrum 2000 FT or 1800 instruments. Solid state ³¹P NMR spectra at 121 MHz were obtained on a Varian Inova 300 instrument using a 4 mm Chemagnetics cross-polarisation, magic angle spinning (CP-MAS) probe. The samples were contained in 4 mm rotors made of partially stabilised zirconia. The spectra were acquired at a spinning speed of 13 kHz with a 120 s delay between pulses and

Table 5 Elemental analyses of platinum complexes^a

	% C	% H	% P
<i>cis</i> -[Pt(κ^2 -C ₆ H ₃ -5-Me-2-PPh ₂) ₂] <i>cis</i> - 2	60.85 (61.21)	4.43 (4.33)	8.25 (8.31)
<i>cis</i> -[Pt(κ^2 -C ₆ H ₃ -6-Me-2-PPh ₂) ₂] <i>cis</i> - 3	61.08 (61.21)	4.25 (4.33)	8.43 (8.31)
<i>trans</i> -[Pt(κ^2 -C ₆ H ₃ -6-Me-2-PPh ₂) ₂] <i>trans</i> - 3	61.28 (61.21)	4.11 (4.33)	8.29 (8.31)
<i>trans,cis,cis</i> -[PtCl ₂ (κ^2 -C ₆ H ₃ -5-Me-2-PPh ₂) ₂] 4	55.97 (55.89)	3.98 (3.95)	7.78 (7.59) ^b
<i>cis,cis,cis</i> -[PtI ₂ (κ^2 -C ₆ H ₃ -5-Me-2-PPh ₂) ₂] 6	45.75 (45.66)	3.46 (3.23)	6.20 (6.20)
<i>trans,cis,cis</i> -[PtI(Me)(κ^2 -C ₆ H ₃ -5-Me-2-PPh ₂) ₂] 7	52.38 (52.77)	4.17 (3.97)	7.05 (6.98)
[Pt ₂ (κ^2 -2-C ₆ H ₄ PPh ₂) ₂ (μ -2-C ₆ H ₄ PPh ₂) ₂] 10	59.90 (60.24)	4.20 (3.90)	8.22 (8.65)
[Pt ₂ (κ^2 -C ₆ H ₃ -5-Me-2-PPh ₂) ₂ (μ -C ₆ H ₃ -5-Me-2-PPh ₂) ₂] 11	59.90 (61.21)	4.36 (4.33)	8.36 (8.31)
[Pt ₂ (κ^2 -C ₆ H ₃ -5-Me-2-PPh ₂) ₂ (μ -C ₆ H ₃ -5-Me-2-PPh ₂) _n] 14	57.40 (61.21)	3.91 (4.33)	8.35 (8.31) ^c
[Pt ₂ (μ -2-C ₆ H ₄ PPh ₂) ₂ (PPh ₃) ₂] 16	59.82 (60.16)	4.09 (4.07)	8.39 (8.63)
[Pt ₂ (μ -C ₆ H ₃ -5-Me-2-PPh ₂) ₂ (PPh ₃) ₂] 17	60.49 (60.65)	4.38 (4.26)	8.76 (8.45)
[Pt ₂ (μ -2-C ₆ H ₄ PPh ₂) ₂ (CNBu ^t) ₂] 18	51.43 (51.20)	4.41 (4.30)	5.48 (5.74) ^d
[Pt ₂ (μ -H)(μ -2-C ₆ H ₄ PPh ₂) ₂ (PPh ₃) ₂]BF ₄ [22]BF ₄	56.43 (56.70)	3.88 (3.90)	8.37 (8.12)
[Pt ₂ (μ -H)(μ -2-C ₆ H ₄ PPh ₂) ₂ (PPh ₃) ₂]CF ₃ SO ₃ [22]OTf	54.49 (55.24)	3.64 (3.75)	7.79 (7.80) ^e
[Pt ₂ (μ -H)(μ -2-C ₆ H ₄ PPh ₂) ₂ (PPh ₃) ₂][MeC ₆ H ₄ SO ₃] [22][<i>p</i> -Tos]	58.42 (58.95)	4.05 (4.13)	7.62 (7.70)
[Pt ₂ (μ -H)(μ -C ₆ H ₃ -5-Me-2-PPh ₂) ₂ (PPh ₃) ₂]PF ₆ [23]PF ₆	55.04 (55.16)	3.82 (3.94)	9.92 (9.61)

^a Calculated values in parentheses. ^b % Cl 8.65 (8.68). ^c % Cl 0.62. ^d % N 2.50 (2.60). ^e % F 3.38 (3.59); % S 1.93 (2.02).

were referenced to external solid NH₄(H₂PO₄) (δ 1.0). Mass spectra were measured on the following instruments: VG ZAB-2 SEQ (FAB using 2-nitrophenyl octyl ether as matrix), HP 5970 MSD (EI), and Bruker Biflex II (MALDI). Elemental analyses were carried out at the Microanalytical Unit of the Research School of Chemistry (ANU) and are listed in Table 5.

The compounds 2-BrC₆H₄PPh₂,⁵¹ 2-Br-4-MeC₆H₃PPh₂,⁷ 2-Br-3-MeC₆H₃PPh₂,⁷ [PtCl₂(SEt₂)₂],⁵² PhICl₂,⁵³ [Pt(PPh₃)_n] (*n* = 3, 4),⁵⁴ and [Pt(PPh₃)₂(η^2 -C₂H₄)]⁵⁵ were prepared by the appropriate literature procedures.

Preparations

cis-[Pt(κ^2 -C₆H₃-5-Me-2-PPh₂)₂], *cis*-**2**. This was prepared from (2-Br-4-MeC₆H₃)PPh₂ (1.143 g, 3.21 mmol), BuⁿLi (2.1 mL of 1.6 M solution in hexanes, 3.36 mmol) and [PtCl₂(SEt₂)₂] (0.638 g, 1.42 mmol) as described for *cis*-**1**.³ After recrystallisation from CH₂Cl₂–methanol, *cis*-**2** was obtained as a white solid (0.868 g, 82%). ¹H NMR (CDCl₃) δ 2.37 (s, 6H, Me), 6.8–7.8 (m, 24H, aromatics), 8.0 (t with br ¹⁹⁵Pt satellites, *J*_{HH} 4.7 Hz, *J*_{PH} 4.7 Hz, *J*_{PH} 55.7 Hz, 2H, *ortho*-H); ³¹P NMR (CDCl₃) δ -52.2 (s, *J*_{PP} 1352 Hz); IR (KBr, cm⁻¹) 3043 m, 2910 m (C–H str), 1565 m (arom C=C str), 724 s (C–H def); EI-MS (*m/z*) 745 [*M*]⁺. X-Ray quality crystals were grown from CH₂Cl₂–methanol.

cis-[Pt(κ^2 -C₆H₃-6-Me-2-PPh₂)₂], *cis*-**3**. This was prepared similarly to *cis*-**2** from (2-Br-3-MeC₆H₃)PPh₂ (1.32 g, 3.72 mmol), BuⁿLi (1.6 M in hexanes, 2.5 mL, 4.00 mmol) and [PtCl₂(SEt₂)₂] (0.696 g, 1.56 mmol). The yield of *cis*-**3**, a white solid, was 0.616 g (53%). ¹H NMR (CDCl₃) δ 2.47 (s, 6H, Me), 6.8–8.0 (m, 26H, aromatics); ³¹P NMR (CDCl₃) δ -62.9 (s, *J*_{PP} 1370 Hz); IR (KBr, cm⁻¹) 3049 m, 2896 m (C–H str), 1562 m (arom C=C str), 724 s (C–H def); EI-MS (*m/z*) 745 [*M*]⁺. X-Ray quality crystals were grown from CH₂Cl₂–pentane.

trans-[Pt(κ^2 -C₆H₃-6-Me-2-PPh₂)₂], *trans*-**3**. A suspension of *cis*-**3** (180 mg, 0.241 mmol) in toluene (20 mL) was heated under reflux for 48 h, during which time the solution became orange. The solution was allowed to cool to room temperature. The resulting white solid was separated by filtration, washed with toluene and pentane and dried *in vacuo* to give *trans*-**3** (112 mg, 62%). ¹H NMR

(CDCl₃) δ 2.07 (s, 6H, Me), 6.8–8.0 (m, 26H, aromatics); ³¹P NMR (CDCl₃) δ -62.9 (s, *J*_{PP} 2445 Hz); EI-MS (*m/z*) 745 [*M*]⁺.

The compound [Pt₂(κ^2 -C₆H₃-6-Me-2-PPh₂)₂(μ -C₆H₃-6-Me-2-PPh₂)₂] **12** was observed *in situ* by ³¹P NMR spectroscopy but it was contaminated with decomposition products and could not be isolated. Its ³¹P NMR parameters are given in Table 2.

[PtXY(κ^2 -C₆H₃-5-Me-2-PPh₂)₂] (X = Y = Cl **4**, Br **5**, I **6**; X = Me, Y = I **7**). To a solution of *cis*-**2** (100 mg, 0.134 mmol) in CH₂Cl₂ (6 mL) was added PhICl₂, Br₂ or I₂ (1 equiv.) in CH₂Cl₂ (6 mL), or neat methyl iodide (1 mL) at room temperature. The solutions were stirred for 30 min, evaporated to dryness, and the residues recrystallised from CH₂Cl₂–methanol. Yields were 80–85%.

trans,cis,cis-**4**. Pale yellow solid; ¹H NMR (CDCl₃) δ 2.47 (s, 6H, Me), 7.0–8.0 (m, 26H, aromatics); ³¹P NMR (CDCl₃) δ -67.7 (s, *J*_{PP} 928 Hz); EI-MS (*m/z*) 779 [*M* - Cl]⁺.

trans,cis,cis-**5**. Pale orange solid, not isolated in a pure state; ³¹P NMR (CDCl₃) δ -74.3 (s, Pt satellites not observed) due to *trans,cis,cis*-**5**, -76.3 (d, *J*_{PP} 5.9 Hz, *J*_{PP} 2081 Hz), -79.7 (d, *J*_{PP} 5.9 Hz, *J*_{PP} 965 Hz) due to *cis,cis,cis*-**5**. Product contaminated with [PtBr₂(κ^2 -C₆H₃-5-Me-2-PPh₂)₂]{ κ^2 -O,C-C₆H₃-5-Me-2-P(O)Ph₂}, 62.9 (s, *J*_{PP} 64.6 Hz), -65.6 (s, *J*_{PP} 2119 Hz); IR (KBr, cm⁻¹) 3039 m, 2953 m (C–H str), 1561 m (arom C=C str), 1064 s (P=O str), 724 s (C–H def); EI-MS (*m/z*) 823 [*M* - Br]⁺, 842 [*M* + O-Br]⁺.

cis,cis,cis-**6**. Orange solid; ¹H NMR (CDCl₃) δ 1.88 (s, 3H, Me), 2.47 (s, 3H, Me), 6.0–8.2 (m, 26H, aromatics); ³¹P NMR (CDCl₃) δ -94.0 (d, *J*_{PP} 7.5 Hz, *J*_{PP} 928 Hz), -98.1 (d, *J*_{PP} 7.5 Hz, *J*_{PP} 991 Hz); EI-MS (*m/z*) 872 [*M* - I]⁺.

trans,cis,cis-**7**. Pale yellow solid; ¹H NMR (CDCl₃) δ 0.92 (t, *J*_{PH} 7.5 Hz, *J*_{PH} 70.9 Hz, 3H, PtMe), 2.41 (s, 6H, Me), 6.8–8.0 (m, 26H, aromatics); ³¹P NMR (CDCl₃) δ -75.7 (s, *J*_{PP} 936 Hz); EI-MS (*m/z*) 887 [*M*]⁺, 760 [*M* - I]⁺.

[PtCl₂(κ^2 -C₆H₃-6-Me-2-PPh₂)₂] **8**. To a solution of *cis*-**3** (100 mg, 0.134 mmol) in CH₂Cl₂ (100 mL) was added PhICl₂ (37 mg, 0.135 mmol) in CH₂Cl₂ (5 mL) and the solution was stirred for 1 min. The solvent was evaporated to a small volume and hexane was added. The resulting pale yellow solid was separated

by filtration, washed with hexane, and dried *in vacuo*. The yield of **8** was 99 mg (90%) and the ratio of *cis*- to *trans*-adducts was typically *ca.* 2 : 1. ^{31}P NMR (CDCl_3) δ -76.9 (s, J_{PtP} 958 Hz) (*trans*-**8**), -76.2 (d, J_{PP} 13.3 Hz, J_{PtP} 2156 Hz) (*cis*-**8**); EI-MS (m/z) 779 [$M - \text{Cl}$] $^+$.

***trans,cis,cis*-[Pt(Me)(κ^2 -C₆H₃-6-Me-2-PPh₂)₂]** **9**. A solution of *cis*-**3** (2 mg, 0.003 mmol) in CD_2Cl_2 (0.7 mL) in an NMR tube was treated with methyl iodide (0.2 mL). The mixture was shaken thoroughly and its ^{31}P NMR spectrum monitored periodically. After 1 h the *trans*-adduct could be detected, together with starting material, but there was extensive decomposition to unidentified products. ^{31}P NMR (CD_2Cl_2) δ -83.9 (s, J_{PtP} 955 Hz) (*trans*-**9**).

[Pt(κ^2 -2-C₆H₄PPh₂)₂(μ -2-C₆H₄PPh₂)₂] **10**. A solution of *cis*-**1** (358.5 mg, 0.50 mmol) in toluene (50 mL) was stirred for 24 h at a bath temperature of 130 °C. The solid had dissolved completely at 80 °C and the colour of the solution slowly changed to yellow. The course of the reaction was monitored by ^{31}P NMR spectroscopy and after 24 h less than 5% of *cis*-**3** remained. The solution was concentrated *in vacuo* to *ca.* 2 mL, transferred to a silica gel column (length 20 cm, internal diameter 3.5 cm), and eluted with toluene-hexane (10 : 1). The first yellow fraction, on evaporation *in vacuo*, gave pure **10** (220 mg, 61%) as a pale yellow powder, mp 286–288 °C, that is soluble in aromatic solvents, THF, ether chloroform and dichloromethane. Solutions in chlorinated solvents slowly decomposed.

[Pt(κ^2 -C₆H₃-5-Me-2-PPh₂)₂(μ -C₆H₃-5-Me-2-PPh₂)₂] **11**. (a) A colourless solution of *cis*-**2** (150 mg, 0.201 mmol) in toluene (30 mL) was heated under reflux for 48 h, during which time a yellow colour developed. The solution was evaporated *in vacuo*, ethanol was added, and the yellow precipitate was separated by filtration, washed with ethanol, and dried *in vacuo*. The yield of **11** was 116 mg (77%). ^1H NMR (C_6D_6) δ 1.80 (s, 6H, Me), 1.84 (s, 6H, Me), 6.4–7.2 (m, 44H, aromatics), 7.94 (dd, J 7.0, 10.5 Hz, 4H, aromatics), 8.14 (dd, J 7.7, 9.9 Hz, 4H, aromatics); MALDI-MS (m/z) 1491 [M] $^+$.

(b) A benzene solution of *cis*-**2** (150 mg, 0.201 mmol) was stirred for 48 h under CO at room temperature, during which time the solution had turned yellow and a fine white precipitate had formed. The latter was removed by centrifugation and the solution was worked up as in (a) to give **11** (60 mg, 40%). The white precipitate, which is insoluble in all common organic solvents, was washed with CH_2Cl_2 and dried *in vacuo* to give 66 mg of product (**14**). The tentative formulation of **14** as a polymeric isomer of *cis*-**2** is based on the ^{31}P -MAS spectrum: δ 19.1 (s, J_{PtP} 2119 Hz), -61.0 (s, J_{PtP} 1118 Hz).

[Pt(CO)(κ -C₆H₃-6-Me-2-PPh₂)(κ^2 -C₆H₃-6-Me-2-PPh₂)₂] **15**. When carbon monoxide was bubbled through a suspension of *cis*-**3** (50 mg, 0.067 mmol) in CH_2Cl_2 (4 mL) for 5 min, the solid immediately dissolved to give an almost colourless solution. Removal of solvent *in vacuo* gave **15** as a white solid (51 mg, 100%); continued pumping led to loss of CO and formation of *trans*-**3**. ^{31}P NMR (CD_2Cl_2) δ -12.3 (d, J_{PP} 2.3 Hz, J_{PtP} 179 Hz, uncoord. P), -62.4 (d, J_{PP} 2.2 Hz, J_{PtP} 1130 Hz, coord. P); IR (KBr, cm^{-1}) 3046 m, 2952 m, 2921 m (C–H str), 2053 s (C \equiv O str), 1566 w (arom C=C str), 723 s (C–H def); EI-MS (m/z) 773 [M] $^+$, 745 [$M - \text{CO}$] $^+$.

The ^{13}C -labelled complex **15a** was prepared similarly. ^{13}C NMR (CD_2Cl_2) δ 22.3, 27.3 (Me), 125–140 (aromatics), 176.6 (dd, J_{PC} 1.4, 3.6 Hz, J_{PtC} 1102, C \equiv O); ^{31}P NMR (CD_2Cl_2) δ -12.5 (br d, J 1.9 Hz due to unresolved J_{PP} and J_{PC} , J_{PtP} 179 Hz, uncoord. P), -62.5 (dd, J_{PP} 2.3 Hz, J_{PC} 3.6 Hz, J_{PtP} 1129 Hz, coord. P); IR (KBr, cm^{-1}) 2004, 1996 ($^{13}\text{C}\equiv\text{O}$ str).

[Pt(μ -2-C₆H₄PPh₂)₂(PPh₃)₂] **16**. A solution containing *cis*-**1** (150 mg, 0.21 mmol) and [Pt(PPh₃)₃] (206 mg, 0.21 mmol) in toluene (20 mL) was stirred for 24 h at 130 °C (bath temperature). The colour changed from orange to red-brown. The solution was concentrated *in vacuo* to *ca.* half-volume and ethanol was added. The precipitated, bright yellow solid was separated by filtration, washed with ethanol (3 \times 30 mL), and dried *in vacuo* to give 231 mg (77%) of **16**, mp 210–214 °C (dec.). The air-stable yellow powder is soluble in aromatic and chlorinated solvents, and in acetone; the solutions in chlorinated solvents decompose slowly.

[Pt(μ -C₆H₃-5-Me-2-PPh₂)₂(PPh₃)₂] **17**. This was prepared similarly to **16** from *cis*-**2** (232 mg, 0.31 mmol) and [Pt(PPh₃)₃] (305 mg, 0.31 mmol) in toluene (30 mL). The product was recrystallised from CH_2Cl_2 -methanol to give **17** as a bright yellow solid (342 mg, 75%). ^1H NMR (C_6D_6) δ 1.73 (s, 6H, Me), 6.4–7.5 (m, 56H, aromatics); MALDI-MS (m/z) 1465 [$M + \text{H}$] $^+$. Crystals suitable for X-ray diffraction were obtained from CH_2Cl_2 -ether.

The reaction time can be shortened to 30 min if [Pt(PPh₃)₂(C₂H₄)] is used in place of [Pt(PPh₃)₃]. Yields are typically 80%.

[Pt(μ -2-C₆H₄PPh₂)₂(CN t Bu)₂] **18**. A solution of **16** (718.1 mg, 0.50 mmol) in toluene (10 mL) was treated in portions with Bu t NC (100.8 mg, 137.1 μL , 1.2 mmol) at room temperature. After *ca.* 10 min the originally cloudy solution became clear and after *ca.* 20 min a pale yellow precipitate of **18** started to appear. The mixture was stirred for 3 h at room temperature, the solvent was removed *in vacuo*, and the residue was washed with THF-hexane (2 : 3) (3 \times 20 mL); it was then dried *in vacuo*. The yield of **18** was 442 mg (82%). ^1H NMR (CD_2Cl_2) δ 1.1 (s, 18H, Me), 6.5–7.9 (m, 28H, aromatics); (C_6D_6) δ 0.74 (Me); ^{13}C NMR (CD_2Cl_2) δ 29.7 (CMe₃), 56.2 (CMe₃), 148 (CNBu t), 128–142 (aromatics); (C_6D_6) δ 29.2 (CMe₃), 55.2 (CMe₃); IR (KBr, cm^{-1}) 2125 vs (C \equiv N str), 1560 w, 725 s.

[Pt(μ -I)(μ -C₆H₃-5-Me-2-PPh₂)₂(PPh₃)₂] **[20]I**. A solution of **17** (200 mg, 0.137 mmol) in CH_2Cl_2 (30 mL) was treated with a solution of iodine (35 mg, 0.138 mmol) in CH_2Cl_2 (15 mL). The mixture was stirred for 10 min and the solvent was removed *in vacuo*. The residue was recrystallised from CH_2Cl_2 -hexanes to give **[20]I** as an orange solid (195 mg, 83%). ^1H NMR (CDCl_3) δ 1.53 (s, 6H, Me), 6.2–7.8 (m, 56H, aromatics); MALDI-MS (m/z) 1592 [$M - \text{I}$] $^+$.

[Pt(μ -H)(μ -2-C₆H₄PPh₂)₂L₂]Y (L = Bu t NC [**21**] $^+$, PPh₃ [**22**] $^+$; Y = various anions). (a) A suspension of **18** (215.4 mg, 0.15 mmol) in ether (15 mL) was treated with HBF₄·OEt₂ (24.3 mg, 0.15 mmol), causing the colour to change from yellow to almost colourless. The slurry was stirred overnight. The solid was separated by filtration, washed with ether (3 \times 20 mL), and dried *in vacuo*. The yield of **[21]BF₄** was 140 mg (80%).

(b) A suspension of **16** (161.8 mg, 0.15 mmol) in ether (15 mL) was treated with HBF₄·OEt₂, CF₃SO₃H or *p*-MeC₆H₄SO₃H

Table 6 Crystal and structure refinement data for *cis*-[Pt(κ^2 -C₆H₃-*n*-Me-2-PPh₂)₂] (*n* = 5, **2**; *n* = 6, **3**), [Pt₂(κ^2 -2-C₆H₄PPh₂)₂(μ -2-C₆H₄PPh₂)₂] **10**, [Pt₂(μ -C₆H₃-5-Me-2-PPh₂)₂(PPh₃)₂] **17** and [Pt₂(μ -H)(μ -C₆H₃-5-Me-2-PPh₂)₂(PPh₃)₂]PF₆ [**23**]PF₆

	2	3	10	17	[23]PF ₆
Chemical formula	C ₃₈ H ₃₂ P ₂ Pt	C ₃₈ H ₃₂ P ₂ Pt	C ₇₂ H ₅₆ P ₄ Pt ₂	C ₇₄ H ₆₂ P ₄ Pt ₂	C ₇₄ H ₆₃ P ₄ Pt ₂ ·PF ₆ ·H ₂ O·0.48C ₆ H ₁₀ O
<i>M</i>	745.71	745.71	1435.31	1465.38	1664.97
Crystal system	Triclinic	Triclinic	Orthorhombic	Monoclinic	Orthorhombic
Space group	<i>P</i> $\bar{1}$	<i>C</i> 2/ <i>c</i>	<i>Ibca</i>	<i>P</i> 2 ₁ / <i>n</i>	<i>Pbca</i>
<i>a</i> /Å	8.9749(1)	21.0147(5)	20.1950(3)	12.6553(1)	16.4610(1)
<i>b</i> /Å	9.0823(1)	9.7799(3)	23.2688(3)	23.2268(2)	34.3557(2)
<i>c</i> /Å	21.0062(3)	15.0753(4)	24.9714(3)	20.6302(2)	25.2509(1)
<i>a</i> /°	96.5555(8)	90	90	90	90
<i>β</i> /°	96.9372(7)	92.0661(12)	90	93.1174(3)	90
<i>γ</i> /°	109.3427(8)	90	90	90	90
<i>U</i> /Å ³	1581.92(4)	3096.29(15)	11 734.4(2)	6055.11(9)	14 280.12(13)
<i>Z</i>	2	4	8	4	8
<i>T</i> /K	200	200	200	200	200
Colour, habit	Colourless diamond shaped plate	Colourless block	Yellow needle	Yellow plate	Colourless needle
Crystal dimensions (mm)	0.30 × 0.20 × 0.10	0.18 × 0.13 × 0.05	0.30 × 0.12 × 0.10	0.14 × 0.10 × 0.07	0.42 × 0.11 × 0.04
<i>D</i> _{calc} /g cm ⁻³	1.565	1.600	1.625	1.607	1.549
μ /mm ⁻¹	4.543	4.661	4.897	4.765	4.09
Total reflections	44 162	28 035	113 538	124 161	138 093
Unique reflections	9261 (<i>R</i> _{int} = 0.08)	3575 (<i>R</i> _{int} = 0.08)	6720 (<i>R</i> _{int} = 0.065)	13 877 (<i>R</i> _{int} = 0.05)	16 360 (<i>R</i> _{int} = 0.06)
Used reflections	7951 [<i>I</i> > 2 σ (<i>I</i>)]	2996 [<i>I</i> > 3 σ (<i>I</i>)]	5589 [<i>I</i> > 3 σ (<i>I</i>)]	8705 [<i>I</i> > 3 σ (<i>I</i>)]	7479 [<i>I</i> > 3 σ (<i>I</i>)]
No. parameters	370	187	352	721	843
<i>R</i> (used reflections)	0.0306	0.0246	0.0398	0.0174	0.0227
Goodness of fit	0.961	1.0817	1.935	1.088	1.079
<i>wR</i> (used reflections)	0.0361	0.0281	0.0534	0.0174	0.0235
ρ _{max} , ρ _{min} /e Å ⁻³	1.19, -1.95	1.65, -1.09	1.89, -1.08	0.43, -0.48	0.69, -0.40

(0.15 mmol) and the mixture was worked up as under (a). The colourless solids [**22**]Y (Y = BF₄⁻, CF₃SO₃⁻ or *p*-MeC₆H₄SO₃⁻) were isolated in 80–90% yield.

[Pt₂(μ -H)(μ -C₆H₃-5-Me-2-PPh₂)₂(PPh₃)₂]PF₆ [**23**]PF₆ (mixture of isomers). To a stirred suspension of **17** (200 mg, 0.137 mmol) in ether (30 mL) was added HPF₆ (60% aq, 1 drop) in ether (5 mL). The yellow colour faded almost immediately. After the mixture had been stirred for 24 h, the colourless solid was separated by filtration, washed with ether and dried *in vacuo*. The yield of [**23**]PF₆ was 215 mg (98%). ¹H NMR (CD₂Cl₂) δ -5.22 (m, *J*_{PH} 6.3, 80.7 Hz, *J*_{PH} 735 Hz, 1H, PtH), 1.57 (s, Me), 2.26 (s, Me), 2.54 (s, Me) (total 6H), 7.0–8.0 (m, 56H, aromatics); ³¹P NMR (CD₂Cl₂) δ 3.0 (P_A) (*J*_{AX} ca. 1700 Hz), 23.5 (P_B) (*J*_{BX} ca. 3900 Hz, *J*_{BX'} ca. 400 Hz); MALDI-MS (*m/z*) 1465 [*M* - PF₆]⁺. X-Ray quality crystals were grown from CH₂Cl₂-ether.

X-Ray crystallography

Data were collected at 200 K on a Nonius-Kappa CCD diffractometer using graphite-monochromated Mo K α radiation (λ = 0.71073 Å) and were measured by means of COLLECT.⁵⁶ Selected crystal data and details of data collection and structural refinement are in Table 6.‡ The intensities of the reflections were extracted and the data were reduced by use of the programs Denzo and Scalepack.⁵⁷ The structures of **2** and **10** were solved by heavy atom Patterson methods (PATTY), expanded by standard Fourier synthesis (DIRDIF 92)⁵⁸ and refined on *F* with use of TEXSAN;⁵⁹ the structures of **3**, **17** and [**23**]PF₆ were solved by direct methods (SIR 92)⁶⁰ and refined on *F* by use of the program CRYSTALS.⁶¹

‡ CCDC reference numbers 645529–645533. For crystallographic data in CIF or other electronic format see DOI: 10.1039/b702808c

Hydrogen atoms attached to carbon atoms were included at idealised positions and ride on those carbon atoms. Where appropriate peaks were observed in difference maps, the methyl groups were oriented to best-fit these peaks, and the other methyl groups were given the same orientations. A peak attributable to the hydride was observed in the structure of [**23**]PF₆. This atom was included and allowed to refine positionally with the restraint that the two Pt–H distances should be equal. This restraint accounts for the small e.s.d.'s associated with the hydride.

The disorder of the phenyl and *p*-tolyl groups in [**23**]PF₆ was evident from the occupancies of less than unity for methyl groups attached to both C(114) and C(134), as well as to C(214) and C(234). The relative occupancies were refined in each case, anisotropic displacement factors being used for the major sites and isotropic for the minor. The ligands containing phosphorus atoms P(3) and P(4) appear to be exclusively triphenylphosphine.

Acknowledgements

Dr David Berry is acknowledged for spectral simulations carried out at the University of Victoria, British Columbia, Canada, the in-house program for which was made available by Dr Keith Dixon. The solid state ³¹P NMR spectra were obtained by Dr James Hook at the University of New South Wales.

References

- 1 F. Mohr, S. H. Privér, S. K. Bhargava and M. A. Bennett, *Coord. Chem. Rev.*, 2006, **250**, 1851, and references cited therein.
- 2 M. A. Bennett, D. E. Berry, S. K. Bhargava, E. J. Ditzel, G. B. Robertson and A. C. Willis, *J. Chem. Soc., Chem. Commun.*, 1987, 1613.
- 3 M. A. Bennett, S. K. Bhargava, M. Ke and A. C. Willis, *J. Chem. Soc., Dalton Trans.*, 2000, 3537.

- 4 M. A. Bennett, S. K. Bhargava, K. D. Griffiths, G. B. Robertson, W. A. Wickramasinghe and A. C. Willis, *Angew. Chem., Int. Ed. Engl.*, 1987, **26**, 258.
- 5 M. A. Bennett, S. K. Bhargava, D. C. R. Hockless, L. L. Welling and A. C. Willis, *J. Am. Chem. Soc.*, 1996, **118**, 10469.
- 6 M. A. Bennett, S. K. Bhargava, K. D. Griffiths and G. B. Robertson, *Angew. Chem., Int. Ed. Engl.*, 1987, **26**, 260.
- 7 S. K. Bhargava, F. Mohr, M. A. Bennett, L. L. Welling and A. C. Willis, *Organometallics*, 2000, **19**, 5628.
- 8 H. H. Hermann, P. Schwerdtfeger, S. K. Bhargava and F. Mohr, *Organometallics*, 2003, **22**, 2373.
- 9 M. A. Bennett and D. L. Milner, *J. Am. Chem. Soc.*, 1969, **91**, 6983.
- 10 J. S. Valentine, *J. Chem. Soc., Chem. Commun.*, 1973, 857.
- 11 D. J. Cole-Hamilton and G. Wilkinson, *J. Chem. Soc., Dalton Trans.*, 1977, 797.
- 12 P. E. Garrou, *Chem. Rev.*, 1981, **81**, 229.
- 13 C. Eaborn, K. J. Odell and A. Pidcock, *J. Chem. Soc., Dalton Trans.*, 1978, 357.
- 14 C. Eaborn, A. Kundu and A. Pidcock, *J. Chem. Soc., Dalton Trans.*, 1981, 933.
- 15 E. Lindner, R. Fawzi, H. A. Meyer, K. Eichele and W. Hiller, *Organometallics*, 1992, **11**, 1033.
- 16 W. P. Power and R. E. Wasylshen, *Inorg. Chem.*, 1992, **31**, 2176.
- 17 M. A. Bennett, S. K. Bhargava, A. M. Bond, A. J. Edwards, S.-X. Guo, S. H. Privér, A. D. Rae and A. C. Willis, *Inorg. Chem.*, 2004, **43**, 7752.
- 18 P. Pykkö, *Chem. Rev.*, 1997, **97**, 597.
- 19 P. S. Pregosin and R. W. Kunz, *³¹P and ¹³C NMR of Transition Metal Phosphine Complexes*, Springer, New York, 1979, pp. 94–96.
- 20 G. K. Anderson, H. C. Clark and J. A. Davies, *Inorg. Chem.*, 1981, **20**, 3607.
- 21 W. J. Cherwinski, B. F. G. Johnson, J. Lewis and J. R. Norton, *J. Chem. Soc., Dalton Trans.*, 1975, 1156.
- 22 B. E. Mann and B. F. Taylor, *¹³C NMR Data for Organometallic Compounds*, Academic, New York, 1981, p. 181.
- 23 G. K. Anderson and R. J. Cross, *Acc. Chem. Res.*, 1984, **17**, 67.
- 24 R. J. McKinney, R. Hoxmeier and H. D. Kaesz, *J. Am. Chem. Soc.*, 1975, **97**, 3059.
- 25 M. A. Bennett, A. M. Clark, M. Contel, C. E. F. Rickard, W. R. Roper and L. J. Wright, *J. Organomet. Chem.*, 2000, **601**, 299.
- 26 H. F. Klein, S. Schneider, M. He, U. Flörke and H. J. Haupt, *Eur. J. Inorg. Chem.*, 2000, 2295.
- 27 W. Keim, *J. Organomet. Chem.*, 1969, **19**, 161.
- 28 D. P. Arnold, M. A. Bennett, M. S. Bilton and G. B. Robertson, *J. Chem. Soc., Chem. Commun.*, 1982, 115.
- 29 Y. Wang, *Huaxue Xuebao*, 1985, **43**, 683.
- 30 N. M. Boag, J. Browning, C. Crocker, P. L. Goggin, R. J. Goodfellow, M. Murray and J. L. Spencer, *J. Chem. Res. (S)*, 1978, (M)2962.
- 31 P. S. Pregosin, *Annu. Rep. NMR Spectrosc.*, 1986, **17**, 285.
- 32 J. Autschbach, C. D. Igna and T. Ziegler, *J. Am. Chem. Soc.*, 2003, **125**, 1028.
- 33 C. Eaborn, K. Odell and A. Pidcock, *J. Chem. Soc., Dalton Trans.*, 1978, 1288.
- 34 M. P. Brown, R. J. Puddephatt, M. Rashidi and K. R. Seddon, *J. Chem. Soc., Dalton Trans.*, 1978, 516.
- 35 J. Jans, R. Naegeli, L. M. Venanzi and A. Albinati, *J. Organomet. Chem.*, 1983, **247**, C37.
- 36 A. R. Siedle, R. A. Newmark and W. B. Gleason, *J. Am. Chem. Soc.*, 1986, **108**, 767.
- 37 R. S. Paonessa and W. C. Trogler, *Inorg. Chem.*, 1983, **22**, 1038.
- 38 L. Abis, A. Sen and J. Halpern, *J. Am. Chem. Soc.*, 1978, **100**, 2915.
- 39 F. Bachechi, *Acta Crystallogr., Sect. C: Cryst. Struct. Commun.*, 1993, **49**, 460.
- 40 F. Bachechi, P. Mura and L. Zambonelli, *Acta Crystallogr., Sect. C: Cryst. Struct. Commun.*, 1993, **49**, 2072.
- 41 F. Bachechi and L. Zambonelli, *J. Organomet. Chem.*, 1983, **250**, 589.
- 42 A. Albinati, S. Chaloupka, J. Eckert, L. M. Venanzi and M. K. Wolfer, *Inorg. Chim. Acta*, 1997, **259**, 305.
- 43 G. Minghetti, A. L. Bandini, G. Banditelli, F. Bonati, R. Szostak, C. E. Strouse, C. B. Knobler and H. D. Kaesz, *Inorg. Chem.*, 1983, 2332.
- 44 M. Capedvila, P. Gonzalez-Duarte, I. Mira, J. Sola and W. Clegg, *Polyhedron*, 1992, **11**, 3091.
- 45 I. Ara, L. R. Falvello, J. Forníes, E. Lalinde, A. Martín, F. Martínez and M. T. Moreno, *Organometallics*, 1997, **16**, 5392.
- 46 A. L. Bandini, G. Banditelli, E. Cesarotti, F. Demartin, M. Manassero and G. Minghetti, *Gazz. Chim. Ital.*, 1994, **124**, 43.
- 47 T. G. Appleton, H. C. Clark and L. E. Manzer, *Coord. Chem. Rev.*, 1973, **10**, 335.
- 48 R. S. Paonessa and W. C. Trogler, *Organometallics*, 1982, **1**, 768.
- 49 G. K. Anderson, *Adv. Organomet. Chem.*, 1993, **35**, 1, and references cited therein.
- 50 *gNMR, Version 4.1 for Windows*, Cherwell Scientific Publishing, Oxford, 1995.
- 51 S. Harder, L. Brandsma, J. A. Kanters, A. Duisenberg and J. van Lenthe, *J. Organomet. Chem.*, 1991, **420**, 143.
- 52 G. B. Kauffman and D. O. Cowan, *Inorg. Synth.*, 1960, **6**, 211.
- 53 H. J. Lucas and E. R. Kennedy, *Org. Synth., Coll. Vol. III*, 1955, 482.
- 54 R. Ugo, F. Cariati and G. La Monica, *Inorg. Synth.*, 1968, **11**, 105.
- 55 U. Nagel, *Chem. Ber.*, 1982, **115**, 1998.
- 56 *COLLECT software*, Nonius BV, Delft, The Netherlands, 1997–2001.
- 57 Z. Otwinowski and W. Minor, in *Methods in Enzymology*, ed. C. W. Carter, Jr and R. M. Sweet, Academic Press, New York, 1997, vol. 276, pp. 307–326.
- 58 P. T. Beurskens, G. Admiraal, G. Beurskens, W. P. Bosman, S. Garcia-Granda, R. O. Gould, J. M. M. Smits and C. Smykalla, The PATTY and DIRDIF Program System, *Technical Report of the Crystallographic Laboratory*, University of Nijmegen, Nijmegen, 1992.
- 59 *TEXSAN, Single Crystal Structure Analysis Software, Version 1.7*, Molecular Structure Corp., The Woodlands, TX, 1992–1997.
- 60 A. Altomare, G. Casciarano, G. Giacovazzo, A. Guagliardi, M. C. Burla, G. Polidori and M. Camalli, *J. Appl. Crystallogr.*, 1994, **27**, 435.
- 61 D. J. Watkin, C. K. Prout, J. R. Carruthers, P. W. Betteridge and R. J. Cooper, *CRYSTALS Issue 11*, Chemical Crystallography Laboratory, Oxford, 2001.
- 62 J. Messelhäuser, M. A. Bennett, S. K. Bhargava, E. J. Ditzel, G. B. Robertson, A. C. Willis and D. E. Berry, *Abstracts of the XIIIth International Conference on Organometallic Chemistry, Turin, September 4–9, 1988*, p. 282.